We are IntechOpen,
the world's leading publisher of
Open Access books
Built by scientists, for scientists

6,900
Open access books available

186,000
International authors and editors

200M
Downloads

Our authors are among the

154
Countries delivered to

TOP 1%
most cited scientists

12.2%
Contributors from top 500 universities

WEB OF SCIENCE™

Selection of our books indexed in the Book Citation Index
in Web of Science™ Core Collection (BKCI)

Interested in publishing with us?
Contact book.department@intechopen.com

Holography: The Usefulness of Digital Holographic Microscopy for Clinical Diagnostics

Zahra El-Schich, Sofia Kamlund, Birgit Janicke,

Kersti Alm and Anette Gjörloff Wingren

Additional information is available at the end of the chapter

Abstract

Digital holographic (DH) microscopy is a digital high-resolution holographic imaging technique with the capacity of quantification of cellular conditions without any staining or labeling of cells. The unique measurable parameters are the cell number, cell area, thickness, and volume, which can be coupled to proliferation, migration, cell cycle analysis, viability, and cell death. The technique is cell friendly, fast and simple to use and has unique imaging capabilities for time-lapse investigations on both the single cell and the cell-population levels. The interest for analyzing specifically cell volume changes with DH microscopy, resulting from cytotoxic treatments, drug response, or apoptosis events has recently increased in popularity. We and others have used DH microscopy showing that the technique has the sensitivity to distinguish between different cells and treatments. Recently, DH microscopy has been used for cellular diagnosis in the clinic, providing support for using the concept of DH, e.g., screening of malaria infection of red blood cells (RBC), cervix cancer screening, and sperm quality. Because of its quick and label-free sample handling, DH microscopy will be an important tool in the future for personalized medicine investigations, determining the optimal therapeutic concentration for both different cancer types and individual treatments.
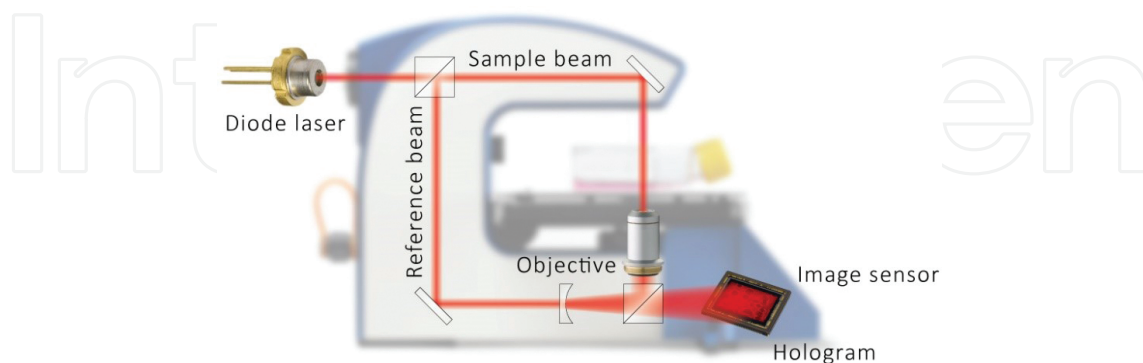
Keywords: cell death, cell volume, digital holographic microscopy, individual treatment

1. Introduction

Digital holographic (DH) microscopy is a digital high-resolution holographic imaging technique with the capacity of quantification of cellular status without any staining or labeling of cells [1–3]. Various cellular parameters can be visualized and calculated from the particular hologram, including individual cell area, thickness, volume, and population confluence and cell counts [4–10]. One of the advantages of studying cells with DH microscopy is that they can be grown and analyzed in their normal growth medium during the entire study. The culture vessel will be placed on the microscope for imaging and then replaced in the 37°C incubator, or placed on a heating plate to retain 37°C, during the analysis. Since the first studies on living cells, DH microscopy has been used to study a wide range of different cell types, e.g., protozoa, bacteria, and plant cells, mammalian cells such as nerve cells, stem cells, various tumor cells, bacterial-cell interactions, red blood cells (RBC), and sperm cells [11–15].

2. Technique

DH microscopy is based on the interference between two, preferably coherent, beams that differ in phase (**Figure 1**). The beams usually originate from the same source, which are split before the sample. One of the beams, the reference beam, will remain undisturbed, while the other, the object beam, will be shifted in phase by the sample. The optical set-up can be either transmissive or reflective, providing no difference in the principle only in the configuration of the optical elements [16]. When the object beam has traveled through or been reflected by the object, the two beams merge. A light detector (e.g., a CCD-sensor) will capture the interference pattern and computer algorithms will convert the signal into a holographic image based on the light phase shifting properties of the cells, the refractive index [17]. The three-dimensional holographic image is then a representation of the real objects [18]. The technique is cell friendly, fast, and simple to use and has unique imaging capabilities for time-lapse investigations on

Figure 1. Schematic view of the DH microscopy technique. A digital holographic setup with a laser beam is split into two identical beams. The sample beam passes through the cells, while the reference beam travels undisturbed. The two beams merge and the image sensor will capture an interference image, which display a 3D-image after reconstruction (www.phiab.se).

both the single cell and the cell-population levels. The reconstructed image contains information about the entire depth of the field of view. For reconstruction to be accurate, the sample has to be transparent and homogenous, where the differences in refractive index between the background and the cells create the tomography of the image [19].

After recording, the hologram consists of the phase and the amplitude of the entire image field. Reconstruction of the image is dependent on the optical configuration, possibly to get rid of optical elements as zero order image and images of other diffraction order. Mathematical algorithms as Fourier transforms or Fresnel transform are usually performed on the wave front [20] .
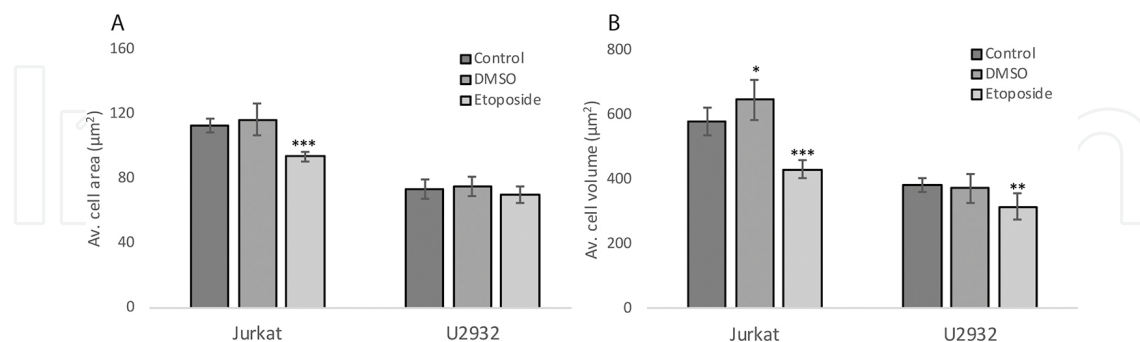
3. Morphological changes connected to cellular events

3.1. Cell death of adherent cells

Cell volume changes, resulting from cytotoxic treatments or apoptosis events, have recently been investigated with DH microscopy [11, 21–25]. When cells go in to early apoptosis, the first discernible indication is an increase in the cell phase shift followed by a decrease as the cell eventually dies [21]. Pavillon et al. recognized early apoptotic cells within minutes by their DH phase signal, while it took several hours to identify dead cells using trypan blue staining [21].

We have previously demonstrated that death-induced cells can be distinguished from untreated cells by the use of DH microscopy [25]. Morphological analyses of the two adherent cell lines L929 and DU145, treated with the anti-tumor agent etoposide for 1–3 days, were performed in cell culture flasks. Etoposide causes errors in the DNA synthesis and promotes apoptosis of the cancer cell by forming a ternary complex with DNA and the enzyme topoisomerase II [26]. Measurements revealed significant differences in the average cell number, the confluence, cell volume, and cell area when comparing etoposide-treated cells with untreated cells. The cell volume of the treated cell lines was initially increased at early time points. By time, cells decreased in volume, especially when treated with high doses of etoposide [25]. Moreover, this analysis was confirmed by a MTS assay. With DH microscopy, small differences between the two cell lines were clarified. Mouse fibroblast L929 cells showed a lower sensitivity for etoposide at the lowest concentrations, while for the human prostate cancer cell line DU145, the confluence, cell area, and volume increased at first, and then decreased over time.

In another study, we selected two suspension cell lines, a diffuse large B-cell lymphoma (DLBCL) cell line, U2932 and the T-cell acute lymphoblastic leukemia cell line Jurkat. The cell lines were treated with dimethyl sulfoxide (DMSO), 100 μM etoposide or left untreated as a control, and were incubated for 24 h. Unpublished work by us shows that the average cell area and cell volume decreased significantly for the Jurkat cell line compared with control. For the U2932 cell line, the average cell area did not change, whereas the average cell volume significantly decreased after etoposide treatment (**Figure 2**). Interestingly, the results may

indicate cell line sensitivity, which also has been shown in the earlier studies [25, 27]. In conclusion, cell death experiments performed with DH microscopy reveal that small differences between two cell lines can be clarified.

Figure 2. Etoposide induces a loss of cell area and volume in the cell lines Jurkat and U2932. Jurkat and U2932 cells were treated with etoposide (100 μM), or left untreated, for 24 h, and holograms were captured by the Holomonitor™ M4. The mean cell area (A) and the mean cell volume (B) were calculated using holographic microscopy images. Error bars are based on the total number of images.
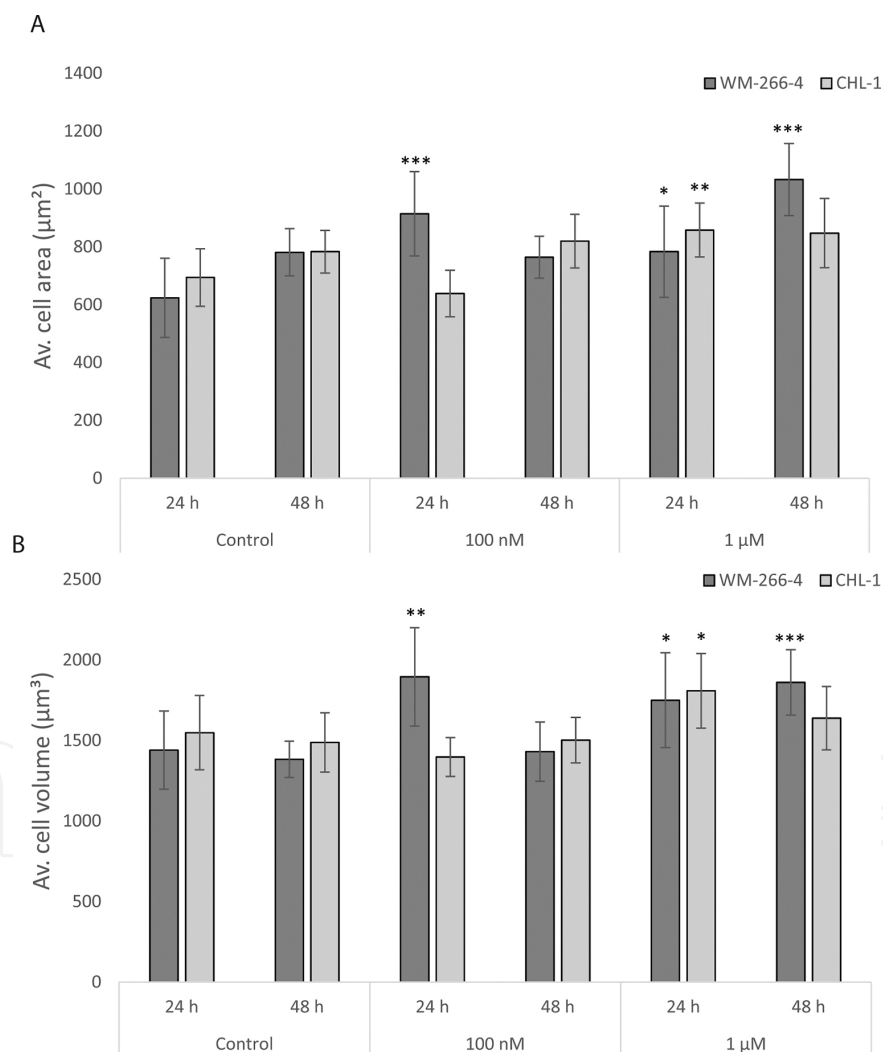
Human α-lactalbumin made lethal to tumor cells (HAMLET) is based on a natural protein present in human breast milk [28]. HAMLET induces cell death in tumor cells and immature cells, but not in normal differentiated cells [29]. As monitored by DH, 15 min of incubation, with 35 μM of HAMLET, was enough for a reduction in cell area and increase in thickness, with evidence of membrane blebbing in human lung carcinoma A549 cells [26]. After 60 min, the cells became even smaller in area and thicker [30]. Puthia et al. examined how HAMLET affects β-catenin and Wnt-signaling in the treated human colon cancer cell line DLD1. Already after 30 min, the cell morphology changed with HAMLET treatment. A time-dependent decrease in cell area and an increase in maximum thickness was seen [31]. DH microscopy was also used to analyze the effect of the cell death-inducing curcumin analog C-150 [32]. Four different glioblastoma cell lines were treated with 1 μM of the analog for 24 h. The results showed significantly increased cell volume and average thickness and decreased cell area for the cell lines investigated.

DH microscopy has been applied for the analysis of chemokinetic responses, selective cytotoxic, adhesion, and migration modulator effects on two different melanoma cell lines, HT168-M1 and A2058, after treatment with di- and trihydroxyanthraquinones [33]. Alizarin and purpurin have been reported to have activity against cancer cells. Their results showed that no basic parameter was influenced by alizarin or purpurin as a cytotoxic or apoptotic substance in HT168-M1 cells. In the case of A2058 cells, alizarin could induce positive effects in the average cell area and volume as measured by DH.

3.2. Cell cycle of adherent cells

Our earlier results on etoposide, colcemid, or staurosporine treated cells showed changes in average cell volume [34]. Mouse fibroblasts were treated and analyzed with DH microscopy after 24 h of incubation. The results showed comparable accuracy to flow cytometry
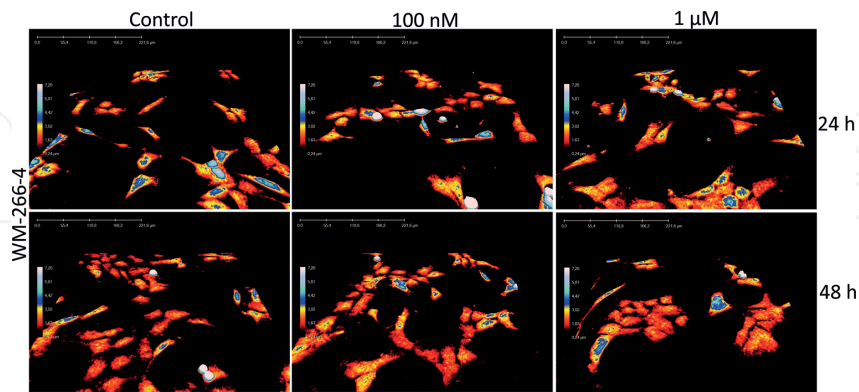
measurement of cell cycle distribution, where staurosporine induced G1 arrest and colcemid or etoposide induced G2/M arrest. The results with DH microscopy showed that the cells decreased in cell size in response to staurosporine treatment, while the cell size increased in response to colcemid or etoposide treatment. Etoposide was further used in a dose-dependent manner in order to investigate how well DH microscopy was able to record a change in the cell cycle profile, as compared to flow cytometry. Etoposide reduced average cell number, decreased average cell confluence, and increased average cell volume. Indeed, using immortalized murine fibroblast cells, this first proof-of-concept study suggests that DH microscopy is a possible alternative tool for analysis of cell cycle alterations [34]. In another study, treated SKOV3-TR cells were visualized for 24 h until cell cycle arrest and characterized by the presence of rounded cells that were unable to complete mitosis [35]. After 44 h, the cells had undergone apoptosis. Higher concentrations of treatment
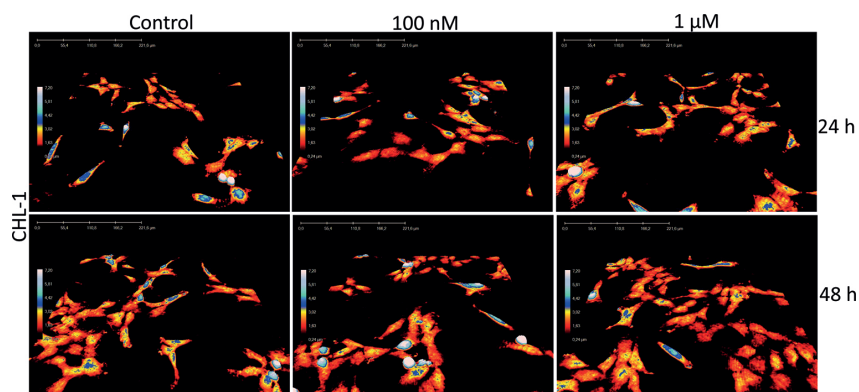

Figure 3. The drug PLX4032 influences cell area and volume differently in the human melanoma cell lines WM-266-4 and CHL-1. WM-266-4 and CHL-1 cells were treated with PLX4032 (100 nM and 1 μM), or left untreated, and holograms were captured by Holomonitor™ M4 after 24 and 48 h, respectively. The mean cell area (A) and the mean cell volume (B) were calculated using holographic microscopy images. Error bars are based on the total number of images.

showed early cell cycle arrest, and the cell population started to undergo apoptosis after 14 h. Indeed, by using time-lapse DH imaging, cell cycle arrest followed by progression to apoptosis was clearly visualized.

Figure 4. 3D-images of WM-266-4 cells. The human skin melanoma cell line WM-266-4 treated with PLX4032 (100 nM and 1 μM), or left untreated. Holograms of the cells were captured using holographic microscopy after 24 and 48 h, respectively. Hologram pictures show the morphology changes over time with the different concentrations of PLX4032.

Figure 5. 3D-images of CHL-1 cells. 3D holograms showing the human skin melanoma cell line CHL-1 treated with PLX4032 (100 nM and 1 μM), or left untreated. Holograms of the cells were captured using holographic microscopy after 24 and 48 h, respectively. Hologram pictures show the morphology changes over time with the different concentrations of PLX4032.
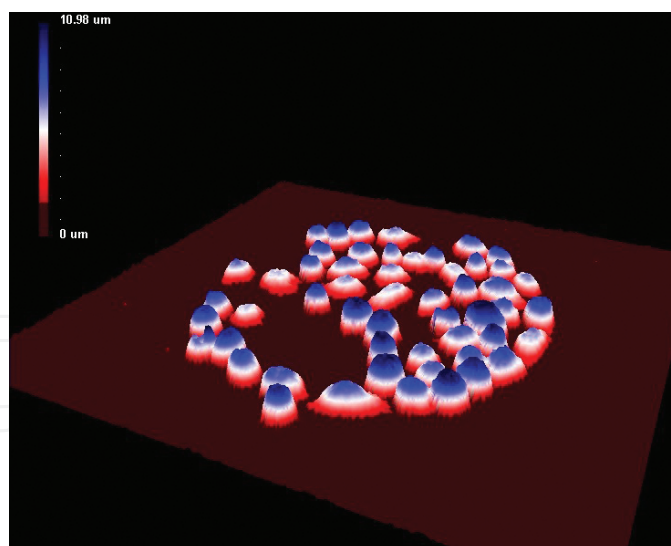
We have treated two human melanoma cell lines, WM-266-4 and CHL-1, with different sensitivity for the drug PLX4032, also called vemurafenib [36]. PLX4032 induces cell cycle arrest in lower doses and apoptosis in higher doses in melanoma cells with a certain *BRAF* gene mutation. It has previously been shown that CHL-1 cells are not inhibited by the drug due to lack of this mutation. In our study, PLX4032 treatment increased the average cell area and cell volume for the WM-266-4 cell line compared with untreated control cells, while the CHL-1 cell line was less affected (**Figure 3**). Morphological cell changes are presented in 3D holograms for WM-266-4 cells (**Figure 4**) and CHL-1 cells (**Figure 5**). The cells become more flat, with increased area, after PLX4032 treatment. Indeed, with DH microscopy, even small differences between treated cells were clarified.

The effect of the novel anti-cancer drug ISA-2011B, etoposide, and docetaxel was monitored with DH microscopy in real-time for up to 48 h by Semenas et al. ISA-2011B treatment led to a reduction in cell size and changes in morphology, which was also achieved by docetaxel treatment [37].

3.3. Cell death of suspension cells on antibody-based microarray

We have introduced antibody-based microarrays [38] to the experimental DH microscopy set-up. By using single-chain variable antibody fragments (scFv) [39], directed against some of the most common cell membrane proteins on T- and B-lymphocytes, suspension cells can be analyzed with DH. Antibody-based microarray techniques have been used to determine phenotypic protein expression profiles for human B cell sub-populations [39] and to detect soluble antigens [40]. In our study [27], we combined DH microscopy and antibody-based microarray to introduce a powerful tool to measure morphological changes in specifically etoposide-treated antibody-captured cells, U2932, and Jurkat (**Figure 6**). We demonstrated that the cell number, mean area, thickness, and volume could be noninvasively measured by using DH microscopy. The cell number was stable over time, but the two cell lines used showed changes of cell area and cell irregularity after treatment. The cell volume in etoposide-treated cells was decreased, whereas untreated cells showed stable volume [27]. In conclusion, cell death of suspension cells investigated with the help of antibody-based microarrays and DH demonstrated that morphological parameters can be investigated of different cell lines and treatments.

Figure 6. Jurkat cells on an antibody-based microarray captured with DH microscopy. A 200,000 Jurkat cells in 100 µl of phosphate-buffered saline (PBS)-0.5% bovine serum albumin were applied to an antibody array and incubated at room temperature for 30 min. The array was thereafter washed manually, until the cell binding areas were clearly visible. A 3D-image was thereafter captured with DH microscopy.

In conclusion, several independent studies now show the feasibility of DH microscopy to demonstrate cell-death induced morphological changes after compound addition.

4. Clinical applications

Lately, DH microscopy is being developed for clinical applications in widely different areas of medicine such as transmembrane water flux, cancer screening, sperm motility, blood cell analysis, and inflammation.

4.1. Transmembrane water flux

In some cases, current imaging techniques are not very well developed. One such example is the measurement of transmembrane water fluxes in epithelial cells directly linked to the activity of a protein involved in cystic fibrosis [41]. DH microscopy was used to quantify the transmembrane water fluxes in situ by determining the phase shift associated with activation of chloride channels. This opens up for the usage of DH microscopy to screen drugs acting on water transporter molecules.

4.2. Cancer screening

Recently, Benzerdjeb et al. reported a preliminary study with DH microscopy as a screening tool for cervical cancer. The study is based on materials from three randomly chosen laboratories, which was analyzed and subjected to DH microscopy. The sensitivity and specificity of DH microscopy was calculated for the detection of neoplasia. The results demonstrated for the first time that the DH microscopy technique is suitable for the processing of gynecologic cervical samples [42].

4.3. Sperm analysis

DH has been used to characterize sperm cells, supplying data for both morphology, motility, and the concentration of the sperm cells, without affecting the sperm reviewed in Ref. [43]. The morphology of the sperm head has often been correlated with the outcome of in vitro fertilization and has been shown to be the sole parameter in semen of value in predicting the success of intracytoplasmic sperm injection and intracytoplasmic morphologically selected sperm injection [44, 45]. Indeed, DH microscopy generates useful information on the dimensions and structure of human sperm, not revealed by conventional phase-contrast microscopy, in particular the volume of vacuoles. This suggests its use as an additional prognostic tool in assisted reproduction technology to better underline the differences between normal and abnormal sperm morphology.

4.4. Blood cell screening

The function of RBCs is strongly connected to their shape, related to different diseases [46]. Therefore, a robust classification method would be of great advantage when analyzing RBC for medical diagnosis and therapeutics. DH microscopy has allowed several investigators to determine vital erythrocyte parameters including morphology and cell counting [15, 47, 48]. Indeed, a DH microscopy-based automated RBC classification method could have the potential for use in drug testing and the diagnosis of RBC-related diseases. Malaria parasites induce

morphological, biochemical, and mechanical changes in RBC. Main clinical diagnostics of malaria is based on microscopic inspection of blood smears, treated with reagents, which stains the malarial parasites. In developing countries, visual identification of malarial RBCs may become unreliable due to lack of sufficiently trained technicians and poor-quality microscopes and reagents. Anand et al. describe the use of quantitative DH microscopy for automatic identification of malaria-infected RBCs by comparing their shape profiles at different axial planes [49]. A correlation algorithm discriminates between the shapes of the cells and determines whether the cell is infected by malaria parasite. Shape comparison is fast and was found to yield fairly accurate discrimination. This technique is mostly advantageous for healthcare personnel working in developing countries. Similarly, other RBC infecting microbes can be investigated, such as *Babesia microti*, which is an obligate parasite in humans, hamster, and mouse. To find alternatives to methods requiring experience of professional technicians, usually based on optical microscope with Giemsa-stained blood smears, DH methodology was exploited [50]. The authors found the technique to be useful for determining morphological modifications in host RBCs, quantifying contents, and concentration of the cellular dry mass, as well as dynamic membrane fluctuations measured at the individual cell level, which are in turn strongly correlated with the mechanical deformability of cell membrane. An automatic compact diagnostic tool will be advantageous especially for healthcare personnel working in developing countries, which lack trained professionals and high-quality equipments.

Platelet spreading and retraction play a pivotal role in the platelet plugging and the thrombus formation. In routine laboratory, platelet function tests include exhaustive information about the role of the different receptors present at the platelet surface without information on the 3D-structure of platelet aggregates. Boudejltia et al. used DH microscopy to develop a convenient method to characterize the platelet and aggregate 3D shapes [51]. This is the first report on analysis of platelets aggregates by DH microscopy. According to the authors, the method is particularly well suited for the study of the platelet physiology, the physiopathology in clinical practice, and the development of new drugs.

4.5. Quantification of inflammation

Lenz et al. have utilized DH microscopy for investigation of inflammatory bowel diseases including Crohn's disease and ulcerative colitis [52]. Dextran sodium sulfate-induced colitis was performed and colonic sections were subsequently examined by histological analyses and by DH microscopy. With DH microscopy, optical path length delay including refractive index was monitored, and thereby tissue density assessment could be performed. Indeed, the average refractive index was an accurate marker to distinguish between different layers of the intestinal wall of the colitis induced murine model.

Furthermore, DH microscopy reliably detects inflamed colonic segments with a strong correlation between the severity of inflammation and the refractive index. In conclusion, DH microscopy analysis opens a novel diagnostic option for optical quantification of inflammation in murine models of colitis. Moreover, the same research group assessed cellular growth and motility in epithelial wound healing in vitro using DH microscopy [53]. Interestingly, phase images quantifying cell thickness, dry mass, and tissue density were demonstrated. The study

concluded that the technique can assist in the evaluation of potential therapeutics in, for example, helping to elucidate the specific role of certain cytokines for wound healing.

5. Conclusion

The correlation between cellular morphological changes and cellular events is rather well documented. In several studies, researchers have shown how holographic cell morphology analysis can be connected to pathological diagnostics. Although the experiments in some cases have been performed ex vivo or in animal models, the analysis of humans is just one small step ahead. For other of the abovementioned applications, experiments are performed with human tissues, and the methods are already beginning to be developed for clinical use. As DH microscopy is noninvasive, the same patient sample can often be used for other analyses, thus adding further benefit to the method.

6. Further research

Future applications could include real-time monitoring of holographic microscopy parameters in human clinical cell samples in response to a broad range of clinically relevant compounds.

Acknowledgements

Author details

Zahra El-Schich[1], Sofia Kamlund[2], Birgit Janicke[2], Kersti Alm[2] and Anette Gjörloff Wingren[1*]

*Address all correspondence to: anette.gjorloff-wingren@mah.se

1 Biomedical Science, Health and Society, Malmö University, Malmö, Sweden

2 Phase Holographic Imaging AB, Lund, Sweden

References

[1] Alm K., Cirenajwis H., Gisselsson L., Gjörloff Wingren A., Janicke B., Mölder A., Oredsson S., Persson J. Digital holography and cell studies. In: Rosen, J., editors. Holography, Research and Technologies. In Tech; Rijeka, Croatia: 2011, pp. 237–252. DOI: 10.5772/15364

[2] Marquet P., Rappaz B., Magistretti P. J., Cuche E., Emery Y., Colomb T., Depeursinge C. Digital holographic microscopy: a noninvasive contrast imaging technique allowing quantitative visualization of living cells with sub wavelength axial accuracy. Optical Society of America. 2005;30(5):468–470. DOI: 10.1364/OL.30.000468

[3] Rappaz B., Marquet P., Cuche E., Emery Y., Depeursinge C., Magistretti P. Measurement of the integral refractive index and dynamic cell morphometry of living cells with digital holographic microscopy. Optical Society of America. 2005;13(23): 9361–9373. DOI: 10.1364/OPEX.13.009361

[4] Carl D., Kemper B, Wernicke G., Bally von G. Parameter-optimized digital holographic microscope for high-resolution living-cell analysis. Applied Optics. 2004;43(36):6536–6544. DOI: 10.1364/AO.43.006536

[5] Chalut K.J., Ekpenyong A.E., Clegg W.L., Melhuisha I.C., Gucka J. Quantifying cellular differentiation by physical phenotype using digital holographic microscopy. Intergrative Biology. 2012;4(3):208–284. DOI: 10.1039/C2IB00129B

[6] Ferraro P., Grilli S., Alfieri D., Nicola S.D., Finizio A., Pierattini G., Javidi B., Coppola G., Striano V. Extended focused image in microscopy by digital holography. Optics Express. 2005;13(18):6738–6749. DOI: 10.1364/OPEX.13.006738

[7] Kemper B., Carl D., Schnekenburger J., Bredebusch I, Schäfer M, Domschke W., Bally von G. Investigation of living pancreas tumor cells by digital holographic microscopy. Journal of Biomedical Optics. 2006;11(3):34005. DOI: 10.1117/1.2204609

[8] Lenart T., Gustafsson M., Öwall V. A hardware acceleration platform for digital holographic imaging. Journal of Signal Processing Systems. 2008;52(3):297–311. DOI: 10.1007/s11265-008-0161-2

[9] Mann C.J., Yu L., Lo C.M., Kim M.K. High-resolution quantitative phase-contrast microscopy by digital holography. Optics Express. 2005;13(22):8693–8698. DOI: 10.1364/OPEX.13.008693

[10] Khmaladze A., Matz R.L., Epstein T., Jasensky J., Banaszak Holl M.M., Chen Z. Cell volume changes during apoptosis monitored in real time using digital holographic microscopy. Journal of Structural Biology. 2012;178(3):270–278. DOI: 10.1016/j.jsb.2012.03.008

[11] Alm K., El-Schich Z, Miniotis M.F., Gjörloff Wingren A., Janicke B., Oredsson S. Cells and holograms–holograms and digital holographic microscopy as a tool to study the

morphology of living cells. In: Mihaylova E., editor. Holography: Basic Principles and Contemporary Applications. In Tech; Rijeka, Croatia: 2013. pp. 335–351. DOI: 10.5772/54505

[12] Marquet P., Depeursinge C., Magistretti P.J .Review of quantitative phase-digital holographic microscopy: promising novel imaging technique to resolve neuronal network activity and identify cellular biomarkers of psychiatric disorders. Neurophotonics. 2014;1(2):020901-1–020901-15. DOI: 10.1117/1.NPh.1.2.020901

[13] Rappaz B., Breton B., Shaffer E., Turcatti G. Digital holographic microscopy: a quantitative label-free microscopy technique for phenotypic screening. Combinatorial Chemistry & High Throughput Screening. 2014;17(1):80–88. DOI: 10.2174/1386207311 3166660062

[14] Nadeau L.J., Cho Y.B., Kühn J., Liewer K. Improved tracking and resolution of bacteria in holographic microscopy using dye and fluorescent protein labeling. Frontiers in Chemistry. 2016;4(17):1–10. DOI: 10.3389/fchem.2016.00017

[15] Yi F., Moon I., Javidi B. Cell morphology-based classification of red blood cells using holographic imaging informatics. Biomedical Optics Express. 2016;7(6):2385-2399. DOI: 10.1364/BOE.7.002385

[16] Kim. M.K. Principles and techniques of digital holographic microscopy. SPIE Reviews. 2010;1:018005. DOI: 10.1117/6.0000006

[17] Xiao X., Puri I.K. Digital recording and numerical reconstruction of holograms: an optical diagnostic for combustion. Applied Optics. 2002;41(19):3890–3899. DOI: 10.1364/AO.41.003890

[18] Sebesta M., Gustafsson M. Object characterization with refractometric digital fourier holography. Optics Letters. 2005;30(5):471–473. DOI: 10.1364/OL.30.000471

[19] Palacios, F., Ricardo, J., Palacios, D., Goncalves, E., Valin, J.L., De Souza, R. 3D image reconstruction of transparent microscopic objects using digital holography. Optics Communications. 2005;248(1–3):41–50. DOI: 10.1016/j.optcom.2004.11.095

[20] Liebling M., Unser M. Comparing algorithms for reconstructing digital off-axis Fresnel holograms. SPIE Proceedings. 2005;6016:6016M. DOI: 10.1117/12.631039

[21] Pavillon N., Kühn J., Moratal C., Jourdain P., Depeursinge C., Magistretti P.J., Marquet P. Early cell death detection with digital holographic microscopy. PloS One. 2012;7(1): 1–9. DOI: org/10.1371/journal.pone.0030912

[22] Wang Y., Yang Y., Wang D., Ouyang L., Zhang Y., Zhao J., Wang X. Morphological measurement of living cells in methanol with digital holographic microscopy. Computational and Mathematical Methods in Medicine. 2013;2013:1–7. DOI: org/10.1155/2013/715843

[23] Trulsson M., Yu H., Gisselsson L., Chao Y., Urbano A., Aits S., Mossberg A.K., Svanborg C. HAMLET binding to α-actinin facilitates tumor cell detachment. PloS One. 2011;6(3): 1–16. DOI: 10.1371/journal.pone.0017179

[24] Kühn J., Shaffer E., Mena J., Breton B., Parent J., Rappaz B., Chambon M., Emery Y., Magistretti P., Depeursinge C., Marquet P., Turcatti G. Label-free cytotoxicity screening assay by digital holographic microscopy. ASSAY and Drug Development Technologies. 2013;11(2):101–107. DOI: 10.1089/adt.2012.476

[25] El-Schich Z., Mölder A., Tassidis H., Härkönen P., Miniotis M.F., Gjörloff Wingren A. Induction of morphological changes in death-induced cancer cells monitored by holographic microscopy. Journal of Structural Biology. 2015;189(3):207–212. DOI: 10.1016/j.jsb.2015.01.010

[26] Montecucco A., Biamonti G. Cellular response to etoposide treatment. Cancer Letters. 2007;252(1):9–18. DOI: 10.1016/j.canlet.2006.11.005

[27] El-Schich Z., Nilsson E., Gerdtsson A.S, Wingren C., Gjörloff Wingren A. Interfacing antibody-based microarrays and digital holography enables label-free detection for loss of cell volume. Future Science OA. 2015;1(3):1–11. DOI: 10.4155/fso.14.2

[28] Fischer W., Gustafsson L., Mossberg A.K., Gronli J., Mork S., Bjerkvig R., Svanborg C. Human α-lactalbumin made lethal to tumor cells (HAMLET) kills human glioblastoma cells in brain xenografts by an apoptosis-like mechanism and prolongs survival. Cancer Research. 2004;64(6):2105–2112. DOI: 10.1158/0008-5472.CAN-03-2661

[29] Svensson M., Håkansson A., Mossberg A.-K., Linse S., Svanborg C. Conversion of alpha-lactalbumin to a protein inducing apoptosis. PNAS. 2000;97(8):4221–4226. DOI: 10.1073/pnas.97.8.4221

[30] Ho J.C.S., Storm P., Rydström A., Bowen B., Alsin F., Sullivan L., Ambite I., MoK K.H., Northen T., Svanborg C. Lipids as tumoricidal components of human alpha-lactalbumin made lethal to tumor cells (HAMLET): unique and shared effects on signaling and death. The Journal of Biological Chemistry. 2013;288(24):17460–17471. DOI: 10.1074/jbc.M113.468405

[31] Puthia M., Storm P., Nadeem A., Hsiung S., Svanborg C. Prevention and treatment of colon cancer by peroral administration of HAMLET (human α-lactalbumin made lethal to tumour cells). Gut. 2014;63(1):131–142. DOI: 10.1136/gutjnl-2012-303715

[32] Hackler Jr. L., Ózsvári B., Gyuris M., Sipos P., Fábián G., Molnár E., Marton A., Faragó N., Mihály J., Nagy L.I., Szénási T., Diron A., Párducz A., Kanizsai I., Puskás L.G. The curcumin analog C-150, influencing NF-κB, UPR and akt/notch pathways has potent anticancer activity in vitro and in vivo. PloS One. 2016;11(3):1–16. DOI: 10.1371/journal.pone.0149832

[33] Lajkó E., Bányai P., Zámbó Z. Targeted tumor therapy by *Rubia tinctorum* L.: analytical characterization of hydroxyanthraquinones and investigation of their selective cyto-toxic, adhesion and migration modulator effects on melanoma cell lines (A2058 and

HT168-M1). Cancer Cell International. 2015;15(119):1–15. DOI: 10.1186/s12935-015-0271-4

[34] Miniotis M.F., Mukwaya A., Gjörloff Wingren A. Digital holographic microscopy for non-invasive monitoring of cell cycle arrest in L929 cells. PloS One. 2014;9(9):1–6. DOI: 10.1371/journal.pone.0106546

[35] Zhang Y., Sriraman S.K., Kenny H.A., Luther E., Torchilin V., Lengyel E. Reversal of chemoresistance in ovarian cancer by co-delivery of a P-glycoprotein inhibitor and paclitaxel in a liposomal platform. Molecular Cancer Therapeutics. 2016;15(10);2282–2293. DOI: 10.1158/1535-7163

[36] Yaktapour N., Meiss F., Mastroianni J., Zenz T., Andrlova H., Mathew N. R., Claus R., Hutter B., Fröhling S., Brors B., Pfeifer D., Milena P.M., Bartsch I., Spehl T.S., Meyer P.T., Duyster J., Zirlik K., Brummer T., Zeiser R. BRAF inhibitor-associated ERK activation drives development of chronic lymphocytic leukemia. The Journal of Clinical Investigation. 2014;24(11):5074–5084. DOI: 10.1172/JCI76539

[37] Semenas J., Hedblom A., Miftakhova R.R., Sarwaa M., Larsson R., Shcherbina L., Johansson M.E., Härkönen P., Sterner O., Persson J.L. The role of PI3K/AKT-related PIP5K1alpha and the discovery of its selective inhibitor for treatment of advanced prostate cancer. PNAS. 2014;111(35):E3689–E3698. DOI: 10.1073/pnas.1405801111

[38] Wingren C., James P., Borrebaeck C.A.K. Strategy for surveying the proteome using affinity proteomics and mass spectrometry. Proteomics. 2009;9(6):1511–1517. DOI: 10.1002/pmic.200800802

[39] Borrebaeck C.A.K., Wingren C. Recombinant antibodies for the generation of antibody arrays. In: Protein Microarrays. Korf U., editor. Humana Press; New York City, USA: 2011. pp. 247–262. DOI: 10.1007/978-1-61779-286-1_17

[40] Belov L., Mulligan S.P., Barber N., Woolfson A., Scott M., Stoner K., Chrisp J.S, Sewell W.A., Bradstock K.F., Bendall L., Pascovici D.S., Thomas M., Erber W., Huang P., Sartor M., Young G.A.R., Wiley J.S., Juneja S., Wierda W.G., Green A.R., Keating M.J., Christopherson R.I. Analysis of human leukaemias and lymphomas using extensive immunophenotypes from an antibody microarray. British Journal of Haematology. 2006;135(2):184–197. DOI: 10.1111/j.1365-2141.2006.06266.x

[41] Jourdain P., Becq F., Lengacher S., Boinot C., Magistretti P.J., Marquet P. The human CFTR protein expressed in CHO cells activates aquaporin-3 in a cAMP-dependent pathway: study by digital holographic microscopy. Journal of Cell Science. 2014;127:546–556. DOI: 10.1242/jcs.133629

[42] Benzerdjeb N., Garbar C., Camparo P., Sevestre H. Digital holographic microscopy as screening tool for cervical cancer preliminary study. Cancer Cytopathology. 2016;124(8):573–580. DOI: 10.1002/cncy.21727

[43] Di Caprio G., Ferrara M.A., Miccio L., Merola F., Memmolo P., Ferraro P., Coppola G. Holographic imaging of unlabelled sperm cells for semen analysis: a review. Journal of Biophotonics. 2015;8(10):779–789. DOI: 10.1002/jbio.201400093

[44] Chra I., Zakova J., Huser M., Ventruba P., Lousova E., Pohanka M. Digital holographic microscopy in human sperm imaging. Journal of Assisted Reproduction and Genetics. 2011;28:725–729. DOI: 10.1007/s10815-011-9584-y

[45] Coppola G., Di Caprio G., Wilding M., Ferraro P., Esposito G.T., Di Matteo L., Dale R., Coppola G., Dale B. Digital holographic microscopy for the evaluation of human sperm structure. Zygote. 2014;22(4):446–454. DOI: 10.1017/S0967199413000026

[46] Yi F., Moon I., Javidi B., Boss D., Marquet P. Automated segmentation of multiple red blood cells with digital holographic microscopy. Journal of Biomedical Optics. 2013;18(2):26006. DOI: 10.1117/1.JBO.18.2.026006

[47] Jaferzadeh K., Moon I. Quantitative investigation of red blood cell three-dimensional geometric and chemical changes in the storage lesion using digital holographic microscopy. Journal of Biomedical Optics. 2015;20(11):111228. DOI: 10.1117/1.JBO. 20.11.111218

[48] Yi F., Moon I., Lee Y.H. Three-dimensional counting of morphologically normal human red blood cells via digital holographic microscopy. Journal of Biomedical Optics. 2015;20(1):016005. DOI: 10.1117/1.JBO.20.1.016005

[49] Anand A., Chhaniwal V.K., Patel N.R., Javidi B. Automatic identification of malaria-infected RBC with digital holographic microscopy using correlation algorithms. IEEE Photonics Journal. 2012;4(5):1456–1464. DOI: 10.1109/JPHOT.2012.2210199

[50] Park H.J., Hong S.H., Kim K., Cho S.H., Lee W.J., Kim Y., Lee S.E., Park Y.K. Characterizations of individual mouse red blood cells parasitized by Babesia microti using 3-D holographic microscopy. Nature Scientific Reports. 2015;5:10827. DOI: 10.1038/srep10827

[51] Boudejltia K.Z., Ribeiro de Sousa D., Uzureau P., Yourassowsky C., Perez-Morga D., Courbebaisse G., Chopard B., Dubois F. Quantitative analysis of platelets aggregates in 3D by digital holographic microscopy. Biomedical Optics Express. 2015;6(9):3556–3563. DOI: 10.1364/BOE.6.003556

[52] Lenz P., Bettenworth D., Krausewitz P., Brückner M., Ketelhut S., von Bally G., Domagka D., Kemper B. Digital holographic microscopy quantifies the degree of inflammation in experimental colitis. Integrative Biology. 2013;5(3):624–630. DOI: 10.1039/C2IB20227A

[53] Bettenworth D., Lenz P., Krausewitz P., Brückner M., Ketelhut S., Domagk D., Kemper B. Quantitative stain-free and continuous multimodal monitoring of wound healing in vitro with digital holographic microscopy. PloS One. 2014;9(9):e107317. DOI: 10.1371/journal.pone.0107317